High speed silicon photonic crystal waveguide modulator for low voltage operation

Lanlan Gu, Wei Jiang,[a),b)] Xiaonan Chen, Li Wang, and Ray T. Chen[a),c)]
Microelectronics Research Center, Department of Electrical and Computer Engineering, The University of Texas, Austin, Texas 78758

(Received 1 December 2006; accepted 14 January 2007; published online 12 February 2007)

A high speed compact silicon modulator is experimentally demonstrated to work at a low driving voltage desirable for on-chip applications. As carrier injection is the only practical option for optical modulation in silicon, a lower limit of current density ($\sim 10^4$ A/cm^2) exists for achieving gigahertz modulation in the *p-i-n* diode configuration. Exploiting the slow group velocity of light in photonic crystal waveguides, the interaction length of this Mach-Zehnder interferometer-type silicon modulator is reduced significantly compared to conventional modulators. The required high current density is achieved with a low voltage (2 V) by scaling down the interaction length to 80 μm. © *2007 American Institute of Physics*. [DOI: 10.1063/1.2475580]

Silicon, the premium material for microelectronics, has long been excluded from the list of favorable photonic materials owing to its intrinsic optical properties. Monolithic integration of microelectronic and photonic devices on a single silicon chip has thus remained a dream for decades. Recent developments in high speed silicon modulators[1,2] and lasers[3,4] showed the great promise of silicon integrated optics. Nonetheless, the voltage and power consumptions of these silicon modulators are too high for on-chip applications, such as optical interconnects.[5] A simple scaling presented below shows that for the most widely employed *p-i-n* diode configuration, these issues for gigahertz modulation stem from a lower limit of ac current density ($\sim 10^4$ A/cm^2) intrinsic to silicon. Photonic crystals,[6,7] periodic lattices on the wavelength scale, have shown the potential to reach the ultimate limit of laser physics in certain devices.[8,9] Here we present a low voltage silicon modulator that achieves high speed modulation in a compact structure by exploiting the slow light effect[10–14] in photonic crystal waveguides.

Interference based conventional wideband silicon modulators, such as Mach-Zehnder interferometers, generally require a dynamically produced critical carrier concentration perturbation on the order of $(\Delta N_e)_c=(\Delta N_h)_c=3\times 10^{17}$ cm^{-3}.[15–20] With this general requirement, we examine the speed scaling of silicon modulators based on *p-i-n* diodes, which represent the predominant electrical configuration for silicon modulators.[2,16–20] Consider an arbitrary optical waveguide whose core dimension is generally on the order of $w_{\text{core}}=1$ μm for wavelengths around 1.55 μm. For moderate to high forward injection, we can generally assume that everywhere in the diode the excess carriers are ultimately supplied externally by the injected current. Regardless of the detailed carrier transport mechanism, the time required to fill the waveguide core to an optically critical level of $(\Delta N_h)_c$ in such a scenario cannot be shorter than

$$\Delta t = q w_{\text{core}} (\Delta N_h)_c / J, \tag{1}$$

where J is the current density and q is the electron charge. Note that a similar form was used to analyze a case where the recombination current prevailed.[16] Also, Eq. (1) reduces to the well-known transit time limit if the drift current dominates. A simple calculation shows that the scaling according to Eq. (1) requires a current density on the order of 10^4 A/cm^2 for a filling time $\Delta t=0.5$ ns. For a conventional waveguide modulator, the cross section for the electric current to pass is given by $A=hL$. Assuming a waveguide height h above 1 μm and a waveguide length L around 1 mm, this requires a current above 0.1 A (a vertical diode setting will reverse h and w_{core} but the conclusion remains the same). Even if a conventional silicon modulator can achieve a low impedance value of 50 Ω, the required power and voltage may yet not be acceptable for most on-chip optical interconnect applications.[5] Scaling down the device dimensions can be the answer to this difficulty. Photonic crystal based structures are capable of shrinking the device interaction length to tens of microns[11–14] and the device height to hundreds of nanometers, which significantly reduces the overall current for the same current density.

The silicon modulator presented here is a Mach-Zehnder interferometer (MZI) based on *p-i-n*-diode-embedded photonic crystal waveguides, as shown in Fig. 1. It was predicted that the interaction length required to obtain a π phase shift for a guided mode is proportional to the group velocity in a waveguide[11] $L\approx(1/2\sigma)(n/\delta n)(V_G/c)\lambda_{\text{air}}$, where σ is the fraction of the total energy of the mode that is stored in the device active region, δn is the perturbation of the material refractive index, V_G is the group velocity of the waveguide, and λ_{air} is the wavelength in air. A significant reduction of L can thus be achieved by taking advantage of a unique property of photonic crystal waveguides (PCWs)—slow group velocity, exhibited over a spectrum range typically 10 nm or wider.[10,11] As to the electrical configurations of silicon modulators, the *p-i-n* diode configuration maximizes the overlap between the optical mode and the nonequilibrium carrier distribution, which enhances the modulation efficiency compared to a metal-oxide-semiconductor (MOS) capacitor.[1] Nevertheless, the *p-i-n* diode based modulators were considered slower than the MOS based modulators.[1] Recent simulations and experiments already revealed that the extraction of carriers under reverse bias was rapid for compact *p-i-n* diode modulators, whereas the slow rising time under forward bias was the primary concern.[2,19]

[a)]Authors to whom correspondence should be addressed.
[b)]Electronic mail: wei.jiang@omegaoptics.com
[c)]Electronic mail: chen@ece.utexas.edu

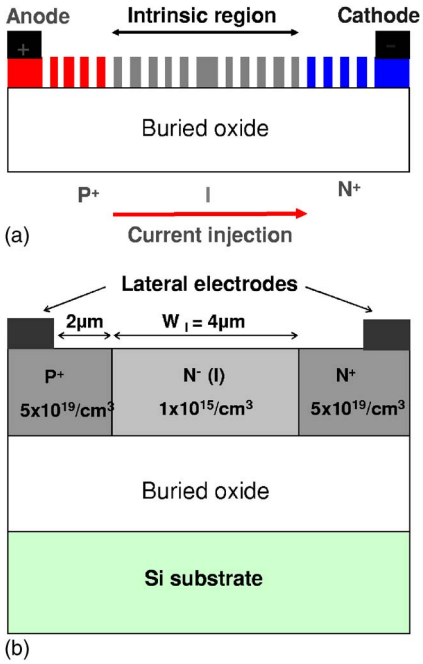

FIG. 1. (Color online) Cross-sectional schematic diagrams of (a) a *p-i-n*-dioded-embedded photonic crystal waveguide and (b) model used in electrical simulation.

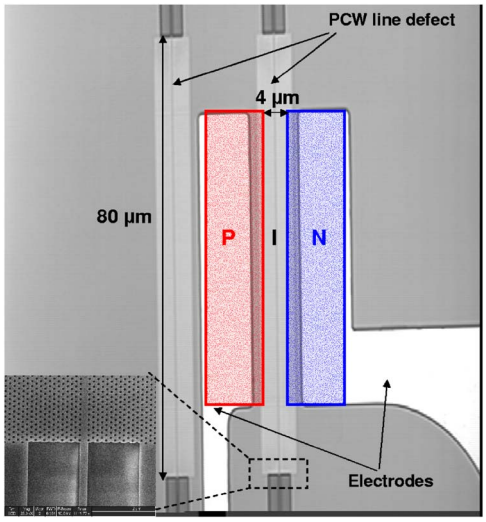

FIG. 2. (Color online) Images of the fabricated device. Microscopic image of a *p-i-n*-diode-based photonic crystal Mach-Zehnder interferometer, where colored overlays indicate the p^+ and n^+ regions. The inset is a scanning electron microscopy image of one end of the photonic crystal waveguide.

The *p-i-n*-diode-embedded PCW MZI modulators were fabricated on a silicon-on-insulator wafer with a 260 nm thick top silicon layer. A strip-waveguide segment in each arm of the MZI was replaced by a line-defect PCW. The PCW was formed in a hexagonal lattice photonic crystal having a period of 400 nm and an air hole diameter of 220 nm. The optical waveguide layer was patterned by electron-beam lithography and drying etching, followed by growing thin thermal oxide up to 7 nm for surface passivation. p^+ and n^+ regions were defined using photolithography and implanted to a concentration about $N_a=N_d=5\times10^{19}$ cm^{-3}. The intrinsic region was n doped to $N_{\mathrm{di}}\sim10^{15}$ cm^{-3}. Careful piranha cleaning of the sample after implantation was found to be crucial for optical loss reduction. The contact windows were opened alongside one of the PCWs by a third photolithography process, and aluminum electrodes were formed by a lift-off process. The contact resistance of the device is about tens of ohms. As the last step, an acrylate-based polymer layer which is transparent at 1.55 μm was coated to cover the device surface. An image of the resulting device is shown in Fig. 2. The overall length of the MZI is around 1 mm, which is mainly determined by the length of two strip-waveguide-based y splitters. However, the overall device length can be reduced to a few tens of microns by using PCW-based y splitters, with additional optimization.

Previous optical simulations have revealed that the energy density of the PCW mode drops by 20 dB at a location about 750 nm away from the PCW central line, which corresponds to a mode width about 1.5 μm.[14] The intrinsic region of the *p-i-n* diode, which covers the entire defect region of a PCW as shown in Fig. 1(b), was designed to be 4 μm wide to ensure an excellent isolation of the guided optical field from the highly absorptive p^+ and n^+ regions. The injection level $J\sim10^4$ A/cm^2 required for gigahertz modulation falls in the high injection regime of a diode, marked by a nonideal static current-voltage relation $I\sim\exp(qV_j/nk_BT)$,[21] where the ideality factor n equals 2 in this nonideal case, V_j is the voltage across the junction, k_B is Boltzmann's constant, and T is the temperature. Fundamentally, this is caused by a "slower" carrier concentration increase with V_j in the form of $\Delta N_e=\Delta N_h=n_i\exp(qV_j/2k_BT)$,[21] where n_i is the intrinsic carrier concentration of silicon. As V_j approaches the contact potential V_0, this gives $\Delta N_e=\Delta N_h=(N_aN_{\mathrm{di}})^{1/2}\sim2.3\times10^{17}$ cm^{-3}, much lower than $\Delta N_h=N_a$ for an ideal diode.

For accurate understanding of the transient carrier transport process, a two-dimensional semiconductor device simulator (MEDICI) was used to model the electrical characteristics of the *p-i-n* modulator. Key physical processes, such as Shockley-Read-Hall recombination, Auger recombination, and impurity-concentration-dependent and field-dependent carrier mobilities, were included in our model. Transient characteristics of the *p-i-n* diode for switching between an on level of 2 V and an off level of −1 V were analyzed, as shown in Fig. 3. Time-dependent electron and hole concentration profiles at the half depth of the top silicon layer are plotted along the device lateral dimension. Note that the profiles vary insignificantly with the depth. Both types of carriers are distributed rather uniformly in most part of the intrinsic region, which produces a quite uniform index perturbation in the entire wave-guiding region and is conducive to the modulation efficiency. More importantly, a filling level of 3×10^{17} cm^{-3}, which induces a refractive index change on the order of 0.001 in silicon,[15] can be reached in the intrinsic region within 0.53 ns after switching on the *p-i-n* diode. With this amount of refractive index change, the slow group velocity of light in our photonic crystal waveguide, designed to give V_g below $0.10c$, further provides up to tenfold reduction of the interaction length from conventional silicon waveguide modulators, pushing it down to the sub-100 μm range.[12,13]

The optical characterization of the *p-i-n* diode based MZI modulator was performed on a fully automated Newport photonics alignment/packaging station. Transverse electric polarized light at a wavelength of 1541 nm was used for optical measurements. Polarization maintaining fibers with a lensed taper end were used to couple the light to and from

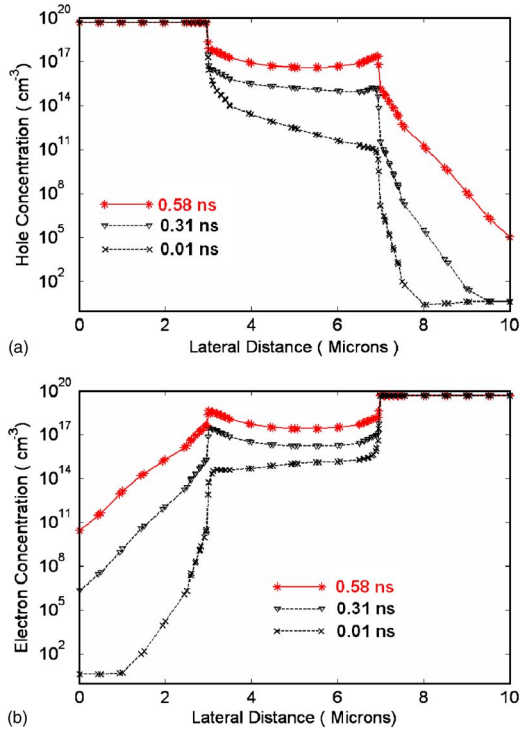

FIG. 3. (Color online) Simulated transient characteristics of the *p-i-n* diode for switching from $V_{off}=-1$ V to $V_{on}=2$ V. Time-dependent distributions of (a) the injected minority carriers (holes) and (b) the injected majority carriers (electrons) along the device lateral dimension within the silicon core layer.

the modulator. As shown in Fig. 4(b) inset, a maximum modulation depth of 93% was obtained at a static injection current of 7.1 mA, which indicates low optical absorption under a forward injection level around 4×10^4 A/cm^2. An Agilent 8133A pulse generator was used to generate the high speed electrical driving signals. Modulated optical signals were detected by a 30 GHz photodetector. Square wave electrical signals having a peak-to-peak amplitude of 3 V ($V_{on}=2$ V, $V_{off}=-1$ V) and a duty cycle of 50% were used for high frequency modulation characterization. The output optical intensities of the modulator at the bit rates of 2 Mbits s^{-1} and 1 Gbit s^{-1} are shown in Fig. 4. Thermo-optic modulation at these high frequencies is estimated to be insignificant compared to electro-optic modulation. A high modulation depth of 85% at 2 Mbits s^{-1} is obtained. The modulation depth is reduced by 3 dB as the modulation frequency increases to 1 Gbit s^{-1}, which marks the 3 dB bandwidth of our device.

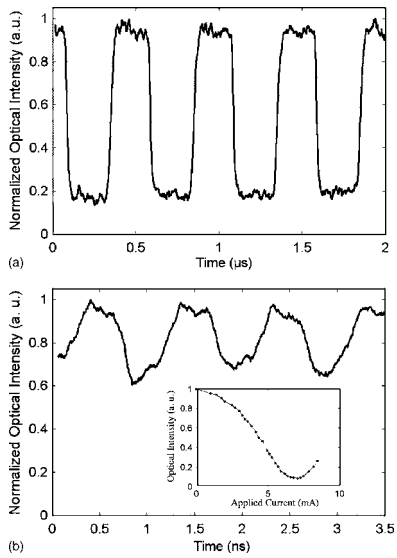

FIG. 4. Modulation measurement results. The normalized output optical intensities of the modulator are shown at (a) 2 Mbits s^{-1} and (b) 1 Gbit s^{-1}. The inset shows the optical intensity at the modulator output as a function of static applied current.

In conclusion, a gigahertz *p-i-n* diode MZI modulator is demonstrated at a low driving voltage desirable for on-chip applications. The interaction length of this device is almost two orders of magnitude shorter than that of a milestone work based on MOS capacitors.[1] Our device is the fastest *p-i-n* diode based MZI modulator ever developed on silicon. Further reducing the intrinsic region width to 1.5 μm is expected to achieve higher modulation speeds with little loss penalty. Differential resistances above 100Ω were measured in the current device under high injection. Further optimization of the device design and fabrication can improve impedance matching and further lower the voltage.

This work is supported in part by AFOSR. The authors are grateful to R. Soref and G. Pomrenke for helpful discussions. The authors thank DARPA for support under the AP2C program. The authors thank the generous support from the State of Texas and Sematech through the AMRC program. The nanofabrication facilities of the Microelectronics Research Center at the University of Texas at Austin are supported in part through NSF's NNIN program. The authors acknowledge partial support of nanocharacterization facilities provided by SPRING.

[1] A. Liu, R. Jones, L. Liao, D. S. Rublo, D. Rubin, O. Cohen, R. Nicolaescu, and Marlo Paniccia, Nature (London) **427**, 615 (2004).
[2] Q. Xu, B. Schmidt, S. Pradhan, and M. Lipson, Nature (London) **435**, 325 (2005).
[3] O. Boyraz and B. Jalali, Opt. Express **12**, 5269 (2004).
[4] H. Rong, A. Liu, R. Jones, O. Cohen, D. Hak, R. Nicolaescu, A. Fang, and M. Paniccia, Nature (London) **433**, 292 (2005).
[5] D. A. B. Miller, Proc. IEEE **88**, 728 (2000).
[6] E. Yablonovitch, Phys. Rev. Lett. **58**, 2059 (1987).
[7] S. John, Phys. Rev. Lett. **58**, 2486 (1987).
[8] O. Painter, R. K. Lee, A. Scherer, A. Yariv, J. D. O'Brien, P. D. Dapkus, and I. Kim, Science **284**, 1819 (1999).
[9] S. Ogawa, M. Imada, S. Yoshimoto, M. Okano, and S. Noda, Science **305**, 227 (2004).
[10] M. Notomi, K. Yamada, A. Shinya, J. Takahashi, C. Takahashi, and I. Yokohama, Phys. Rev. Lett. **87**, 253902 (2001).
[11] M. Soljacic, S. G. Johson, S. Fan, M. Ibanescu, E. Ippen, and J. D. Joannopoulos, J. Opt. Soc. Am. B **19**, 2052 (2002).
[12] Y. A. Vlasov, M. O'Boyle, H. F. Hamann, and S. J. McNab, Nature (London) **438**, 65 (2005).
[13] Y. Jiang, W. Jiang, L. Gu, X. Chen, and R. T. Chen, Appl. Phys. Lett. **87**, 221105 (2005).
[14] L. Gu, Y. Jiang, W. Jiang, X. Chen, and R. T. Chen, Proc. SPIE **6128**, 261 (2006).
[15] R. A. Soref and B. R. Bennett, IEEE J. Quantum Electron. **23**, 123 (1987).
[16] G. V. Treyz, P. G. May, and J. Halbout, Appl. Phys. Lett. **59**, 771 (1991).
[17] C. Z. Zhao, G. Z. Li, E. K. Liu, Y. Gao, and X. D. Liu, Appl. Phys. Lett. **67**, 2448 (1995).
[18] P. Dainesi, A. Kung, M. Chabloz, A. Lagos, Ph. Fluckiger, A. Ionescu, P. Fazan, M. Declerq, Ph. Renaud, and Ph. Robert, IEEE Photonics Technol. Lett. **12**, 660 (2000).
[19] A. A. Barrios, V. R. Almeida, and M. Lipson, J. Lightwave Technol. **21**, 1089 (2003).
[20] A. Irace, G. Breglio, and A. Cutolo, Electron. Lett. **39**, 232 (2003).
[21] B. G. Streetman and S. Banerjee, *Solid State Electronic Devices* (Prentice-Hall, Upper Saddle River, NJ, 2000), p. 213.